Physica 6D (1982) 78–94
North-Holland Publishing Company

THE AUTOCORRELATION FUNCTION OF A PSEUDOINTEGRABLE SYSTEM

Frank S. HENYEY and Neil POMPHREY
Center for Studies of Nonlinear Dynamics of La Jolla Institute, P. O. Box 1434, La Jolla, California 92038, USA

Received 30 December 1981
Revised 8 April 1982

The autocorrelation function of a pseudointegrable system is considered. The system consists of "billiards" on a plane surface formed out of three squares arranged in an "L" shape. This system has the important property of being constructed from copies of an integrable subsystem, the single square. The motion can be decomposed into a continuous and a discrete part, the unpredictability in the system being associated with the latter. A discrete autocorrelation function is calculated, and its decay properties investigated. Structure found in this autocorrelation function is associated with the continued fraction expansion of the ratio of velocity components. For repeating continued fractions, such as the golden mean, the autocorrelation function exhibits a selfsimilar structure. For the general case of a randomly chosen velocity ratio, we derive the time dependence of the number of occurrences of "large" autocorrelation values, which differs from the behavior in integrable and chaotic systems.

1. Introduction

Zemlyakov and Katok [1], Casati and Ford [2], and Richens and Berry (RB, [3]) have drawn attention to a special class of N-degree of freedom dynamical systems. Following RB, we refer to these systems as "pseudointegrable." They have properties commonly associated with *both* integrable and nonintegrable systems, as well as special properties of their own.

Pseudointegrable systems possess N constants of the motion which restrict the dynamics to lie on an N-dimensional invariant manifold of the $2N$-dimensional phase space (cf. integrable systems), however, the topology of the manifold is different from a torus. This is possible (in view of a topological theorem due to Arnol'd [4]) because of the existence of singular points of the phase flow which lie on multiply-handled spheres. RB suggest that no generalization of action-angle variables can be defined for pseudointegrable systems because of the "splitting" of beams of trajectories near the singular points. If a trajectory were to encounter a singular point there would be no unique continuation of the trajectory. If such a point is isolated on the N-dimensional manifold (or, more generally, if the point lies on a codimension ≥ 2 invariant subset of phase space) the probability of a randomly chosen trajectory ever intersecting it is zero.

The pseudointegrable system we investigate is described in section 2 (see RB for other such systems). It constitutes a problem in "billiard" dynamics, the singular points of the phase flow arising from the possible encounters of the billiard ball with an interior 270° corner. Pseudointegrable systems, however, are not restricted to collision dynamics: Motion along geodesics of a cone (with some means of return) is an example. Here the apex of the cone provides the singular point of the flow.

Beam splitting has often been used to distinguish integrable from chaotic behavior: Most nearby trajectories of integrable systems separate no faster than linearly at long times. In chaotic systems, however, nearby trajectories separate exponentially with time. Pseudointegrable systems have an intermediate behavior: Separation of adjacent trajectories is linear, $d \sim$

$k_1 t$, until such time as a singular point divides them. After this time, the trajectories move to distant points in phase space (so their separation is comparable to the diameter D of phase space). The number of encounters (approaches to within some small distance R) of the beam with the singularity grows linearly, $n \sim k_2 t$, so that the probability that the singularity has divided any pair of trajectories is

$$\frac{nd}{R} = \frac{k_1 k_2}{R} t^2.$$

The expected value of the separation is simply D times this probability, which grows like t^2. (See also discussion in Hobson [5]).

The faster than linear separation implies a degree of unpredictability in one's ability to correlate trajectory pairs over long times. In the particular type of pseudointegrable system we will consider, this unpredictability is of a simple kind. Our system is constructed by tesselation of integrable subsystems. In particular, we consider billiards on a plane surface formed out of three squares arranged in an "L" shape (see fig. 1). The phase point of the pseudointegrable system is uniquely specified by the phase space point of the associated integrable system together with an integer j between 1 and N_c. Phase space may be thought of as N_c copies of the integrable system. Motion within each copy is according to the integrable laws of motion, with rules for transitions between equivalent points of different copies. The singularity is due to a discontinuity in the transition rule. The unpredictability of the system is due to the (discrete) unpredictability of the integer labelling the copy. Numerical integration of such a pseudointegrable system is straightforward. We explicitly integrate the integrable system, and, in terms of this solution, apply the transition rules. This is a discrete problem and is not plagued with roundoff errors as are most calculations of nonintegrable systems.

In this paper, we present a numerical investigation of the classical autocorrelation function of a pseudointegrable system. The behavior of autocorrelation functions of generic integrable Hamiltonian systems is known: Casati, Valz-Gris, and Guarneri [6] have shown that the microcanonical autocorrelation function of any smooth phase space function will decay to its final value as $\tau^{(1-N)/2}$, where N is the number of degrees of freedom. Casati et al. point out that "typical" behavior of correlation functions of nonintegrable systems is unknown, and it may prove to be the case that *no* typical behavior exists. In the work to be reported here, no attempt is made to average over initial conditions.

In section 3 it is shown that the autocorrelation function of position $x(t)$ can be decomposed into two parts. The first of these is periodic and fully determined. The second is a convolution between a known function and a discrete autocorrelation function, $A_D(\tau)$, whose properties we would like to understand.

Specification of the dimensionless ratio of velocity components, $|v_x/v_y|$, is sufficient to determine the dynamics. Section 4 is a presentation of a numerical calculation of $A_D(\tau)$ for the case when the velocity ratio equals the golden mean $(\sqrt{5}+1)/2$. A self-similar pattern is found whose details depend on understanding the behavior of the system for rational values of $|v_x/v_y|$.

In section 5 we consider the periodic orbits of the pseudointegrable system. These are obtained for the initial conditions $|v_x/v_y| = p/q$, with p and q relatively prime. If the orbit were restricted to a single square, a time scale could be defined such that the period would be p. For the 3-square pseudointegrable system, the orbit may have period p, $2p$, or $3p$ depending on the parity of p and q. The prescription for which of these is appropriate is given. The behavior of the discrete autocorrelation function for the case of periodic motion is described.

Section 6 deals with the case of irrational velocity ratios. On the basis of some computer

calculations of the autocorrelation function, certain patterns emerge from the results. These can be understood using two elementary principles. The first of these relates the behavior of $A_D(\tau)$ for irrational $|v_x/v_y|$ to the behavior for certain rational approximations to $|v_x/v_y|$. It is the continued fraction expansion of the velocity ratio that provides the relevant rational approximations. The second principle relates correlations at two time differences τ_1, and τ_2, say, to induced correlations at $\tau = \tau_1 \pm \tau_2$. This second principle is evidenced by a bound that can be demonstrated for the 3-square system. When the orbit decorrelation, $A_D(0) - A_D(\tau)$, is small, an analytic estimate of $A_D(\tau)$ is possible.

We close the paper with a prediction in section 7 of the behavior of the autocorrelation function for a randomly chosen, i.e., typical, initial condition. The predicted behavior contrasts with the behavior associated with integrable and with chaotic systems.

2. System description

We consider a particularly simple pseudointegrable system, one of a class described in [3], "billiards" on a table made out of three congruent squares as shown in fig. 1. The particle travels in a straight line with constant speed in the interior of the table and undergoes specular reflection off the sides. A segment of a typical trajectory is shown in the figure. Phase space consists of the position on the table and the values of v_x and v_y. The conserved quantities are v_x^2 and v_y^2 (where the axes are parallel to the sides of the squares). Thus the accessible phase space is two dimensional and consists of four copies of the table, one for each choice of the pair of signs of v_x and v_y. These four copies can be arranged by reflection and joined in such a way that the velocity is always upward toward the right, and the trajectory moves in a continuous straight line across the joints between the copies. Fig. 2 shows this arrangement, including the same segment of trajectory shown in fig. 1.

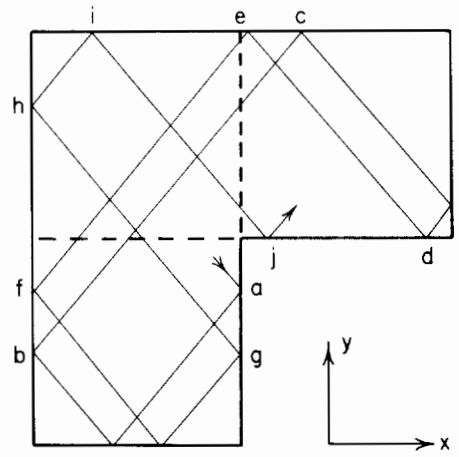

Fig. 1. The three-square billiard. A particle bounces specularly off the walls. A portion of a trajectory is labelled to facilitate comparison with subsequent figures. We are considering the autocorrelation function for the coordinate "x" whose direction is shown.

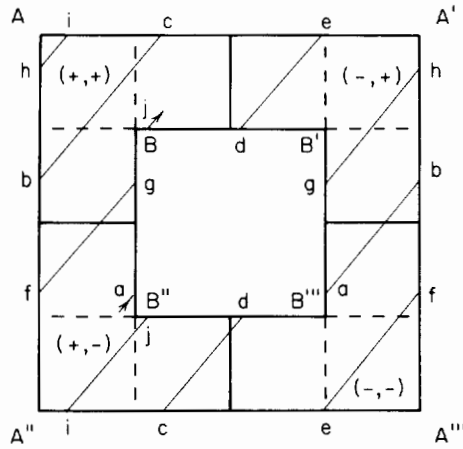

Fig. 2. The invariant manifold consisting of twelve squares, formed by joining four copies of the 3-squares, one for each sign combination of v_x, v_y. The trajectory shown is the same as that of fig. 1, as are the points $a, b, \ldots, j$.

The phase trajectory is a straight line on the space made by identifying appropriate sides. The side AA' is identified with $A''A'''$, the side AA'' with the side $A'A''$, BB' with $B''B'''$, and BB'' with $B'B'''$. Identifying the A sides leads to a torus with a square hole, and joining the B

sides puts a handle on that torus, leading to a genus 2 surface. The point $B = B' = B'' = B'''$ is the singular point at which an emerging trajectory can leave in two ways. Thus if a trajectory intersects BB'' an infinitestimal distance above B'' it emerges near B''', but if it intersects $B''B'''$ infinitesimally to the right of B'' it emerges near B. If fig. 2 is folded along all lines, the twelve squares lie on top of one another, and the motion on the single square is simply the integrable case of billiards in a square. We integrate the equations of motion for the pseudointegrable system by using the trivial solution for billiards in a single square and by following the sequence of squares that are occupied.

3. The discrete autocorrelation function

Let $x(t)$ denote the distance measured parallel to the top and bottom sides of the squares. The autocorrelation function of $x(t)$ is

$$A(\tau) = \langle x(t)x(t+\tau)\rangle \equiv \lim_{T\to\infty}\frac{1}{T}\int_0^T x(t)x(t+\tau)\,dt. \quad (1)$$

If the system were comprised of a single square, $x(t)$ would be periodic, and therefore $A(\tau)$ would be periodic with the same period. We choose this period to define the unit of time. By selecting a single angle variable $x(t)$ as phase space function, unnecessary detail caused by multiple periodicity of the autocorrelation function is avoided, and we can concentrate on features of the autocorrelation function that are due to the pseudointegrability of the system.

Fig. 3a shows $x(t)$ for the trajectory drawn in figs. 1 and 2. It is clear that $x(t)$ is the convolution between the triangle function

$$T(x) = \begin{cases} 1-2|x| & \text{for } |x| \leqslant \frac{1}{2}, \\ 0 & \text{for } |x| \geqslant \frac{1}{2}, \end{cases} \quad (2)$$

and a set of delta functions

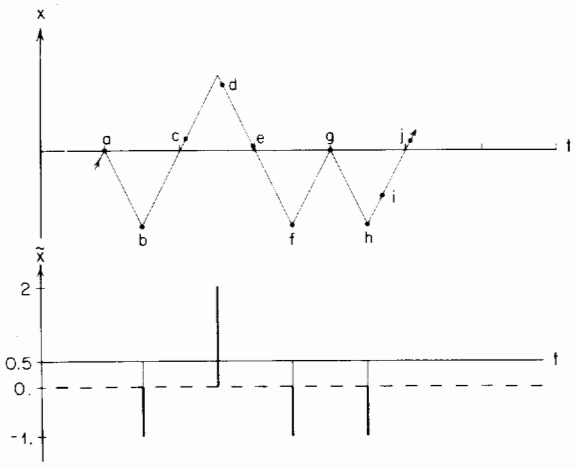

Fig. 3. a) $x(t)$ for the trajectory shown in figs. 1 and 2, with points $a, b, \ldots, j$ from these figures. $x(t)$ consists of a sequence of congruent triangles. b) The deconvolution D' of the same $x(t)$ and a single triangle, $x = D' * T$. The coefficients d_n' and positions of the delta functions comprising D' are shown, relative to the solid horizontal axis. The quantities $d_n = d_n' + \frac{1}{2}$ are shown relative to the dashed line. The mean $\langle d_n\rangle$ is zero.

$$D'(t) = \sum_n d_n'\delta(t-n). \quad (3)$$

The weights d_n' have magnitude equal to the length of a side of a square, which we normalize to be 3/2 for convenience, and the spacing between the delta functions is one unit of time (defined above). $D'(t)$ is represented in fig. 3b, where the weight of each delta function is given by the displacement from the solid horizontal axis. The displacement is positive for a collision with the upper right wall, and negative for a collision with a left wall.

As is usually the case, it is most convenient to remove the mean from the function whose correlation is being calculated. Define

$$d_n = d_n' - \langle D'\rangle, \quad (4)$$

$$D(t) = \sum_n d_n\delta(t-n),$$

and

$$R(t) = \langle D'\rangle\sum_n(\delta(t-n)-1).$$

Then

$$x(t)-\langle x\rangle = D*T + R*T. \tag{5}$$

The autocorrelation function of $x(t)-\langle x\rangle$ is therefore the sum of the autocorrelations of two functions with zero mean. Consider first the autocorrelation of $R*T$. For a single square of side 3/2, $x(t)-\langle x\rangle$ is the convolution of

$$\tfrac{3}{2}\sum_n(\delta(t-n)-1)$$

with T. Therefore $R*T$ is $2/3\langle D'\rangle$ times $x(t)-\langle x\rangle$ for a single square, and its autocorrelation function is

$$A_{R*T} = \frac{4\langle D'\rangle^2}{9}A_{\text{Single Square}}. \tag{6}$$

For the 3-square system, $\langle D'\rangle = -\frac{1}{2}$, and

$$A_{R*T} = \tfrac{1}{9}A_{\text{Single Square}}.$$

We call A_{R*T} the "deterministic" part of A since it has a correspondence with integrable motion. It is a periodic function of τ with a period of one time unit. Specifically,

$$A_{R*T} = \frac{1}{24}\left(16\left(\tau-\frac{1}{4}\right)^3 - 3\left(\tau-\frac{1}{4}\right)\right), \quad \text{for } 0\leq\tau\leq\tfrac{1}{2}, \tag{7}$$

and is symmetric about $\tau = 0$ and about $\tau = \frac{1}{2}$.

Now consider the autocorrelation of $D*T$,

$$A_{D*T} = A_D * A_T. \tag{8}$$

The function $A_T(\tau)$ is found to be

$$A_T(\tau) = \begin{cases} \frac{1}{3}-2|\tau|^2+2|\tau|^3, & \text{for } |\tau|\leq\frac{1}{2}, \\ \frac{2}{3}(1-|\tau|)^3 & \text{for } \frac{1}{2}\leq|\tau|\leq 1, \\ 0 & \text{for } 1\leq\tau, \end{cases} \tag{9}$$

which is almost indistinguishable from a Gaussian of the same area and width. $A_D(\tau)$ consists of a set of delta functions at integer values of τ, where the weight of each delta function is the value of the discrete time series made up of the weights of the delta functions in $D(t)$. In other words,

$$D(t) = \sum_n d_n\delta(t-n),$$

and

$$A_D(\tau = n) = \lim_{N\to\infty}\frac{1}{2N}\sum_{m=-N}^{N} d_m d_{m+n}. \tag{10}$$

Hence

$$A_{D*T}(\tau) = \sum_m A_D(m)A_T(\tau-m). \tag{11}$$

Since $A_T(\tau)$ has support on $|\tau|<1$, exactly two terms contribute at each value of τ, except for integer values, at which only one term contributes.

The decomposition of the autocorrelation function of $x(t)-\langle x\rangle$ into a periodic deterministic part and a part which takes on values at discrete time intervals is made possible by the reduction of the system into integrable and discrete subsystems. We believe that the periodic part would not be present for a more general pseudointegrable system but would be replaced by a decaying contribution. Whatever is the case, A_{D*T} is more likely to exhibit generic structure and will be the subject of the investigations in this paper. Since the convolution of A_D with A_T contains no physics, we will ignore this convolution and concentrate on properties of the discrete autocorrelation function $A_D(\tau)$. Aside from a factor of $\frac{1}{3}$, this function has the same value as $A_{D*T}(\tau)$ at integer values of τ.

Most* trajectories will fill all three squares of

*With the exception of a set of initial conditions of zero Liouville measure.

the system uniformly. Therefore $d'_n = -\frac{3}{2}$ twice as often as $d'_n = +\frac{3}{2}$, and $\langle D' \rangle = -\frac{1}{2}$. It follows that d_n takes on the values -1 and 2 and that $\langle D \rangle = 0$. $D(t)$ is represented in fig. 3b, where the weights are given by the displacements from the dashed horizontal axis. Without recourse to numerical experiments it is difficult to be specific as to the values of $A_D(\tau)$ for given τ. However, the value $A_D(0)$ is easily calculated to be

$$A_D(0) = \tfrac{1}{3}(2)^2 + \tfrac{2}{3}(-1)^2 = 2. \tag{12}$$

It is normalized at twice the conventional value of unity. For most* trajectories we can also evaluate $A_D(1)$, based on the observation that if $d_n = 2$ then $d_{n\pm1} = -1$, since the trajectory can not remain in the upper right square for more than one time unit. In order for $d_n = -1$ to occur twice as often as $d_n = +2$ (to give $\langle D \rangle = 0$), the transitions $d_n = -1$, $d_{n+1} = 2$; $d_n = 2$, $d_{n+1} = -1$; and $d_n = -1$, $d_{n+1} = -1$ must all occur with equal frequency. Thus

$$A_D(1) = \tfrac{1}{3}(-2) + \tfrac{1}{3}(-2) + \tfrac{1}{3}(1) = -1. \tag{13}$$

$A_D(0) = 2$ and $A_D(1) = -1$ represent an upper and lower bound to $A_D(\tau)$ for any τ (see appendix).

4. Self-similar autocorrelation function

Our first numerical experiments were performed using an Apple™ personal computer, a system with superior graphics capabilities. In this section the results of one of these early experiments are summarized.

The parameter that determines the dynamics, and also therefore the autocorrelation function, is the ratio of velocity components, $|v_x/v_y|$, which is a constant. The first numerical runs were for $|v_x/v_y| = (\sqrt{5}+1)/2$, the "golden mean." A plot of the discrete autocorrelation function $A_D(\tau)$ at the first 2000 time values is shown in fig. 4. Although there are hints of structure, the details are unclear. However, the repeated application of a simple smoothing algorithm

$$A_D(\tau) := \tfrac{1}{4}(|A_D(\tau-1)| + 2|A_D(\tau)| + |A_D(\tau+1)|) \tag{14}$$

results in fig. 5, obtained after twenty iterations. A self-similar pattern is evident: Each peak, centered at $\tau = 21$, 89, 377, 1597, is half the height of the peak at $\tau = 0$. The smaller peaks at $\tau = 89 \pm 21$; 377 ± 21, 377 ± 89; 1597 ± 377, etc., are again half the size of the parent. The next generation (e.g., $1597 \pm 377 \pm 21$) is half these. By examining the original (unsmoothed) data we

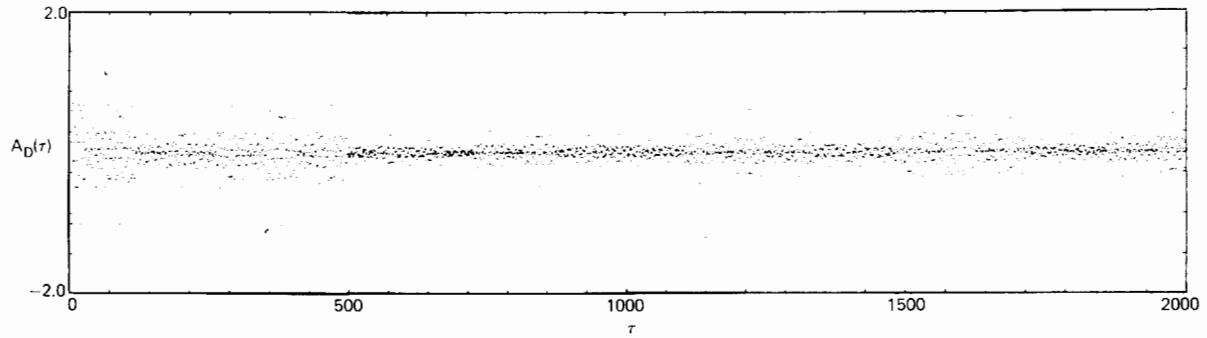

Fig. 4. The discrete autocorrelation function $A_D(\tau)$ for $0 \leq \tau \leq 2000$, shown for $|v_x/v_y|$ = golden mean. The structure of A_D is not very apparent in this presentation.

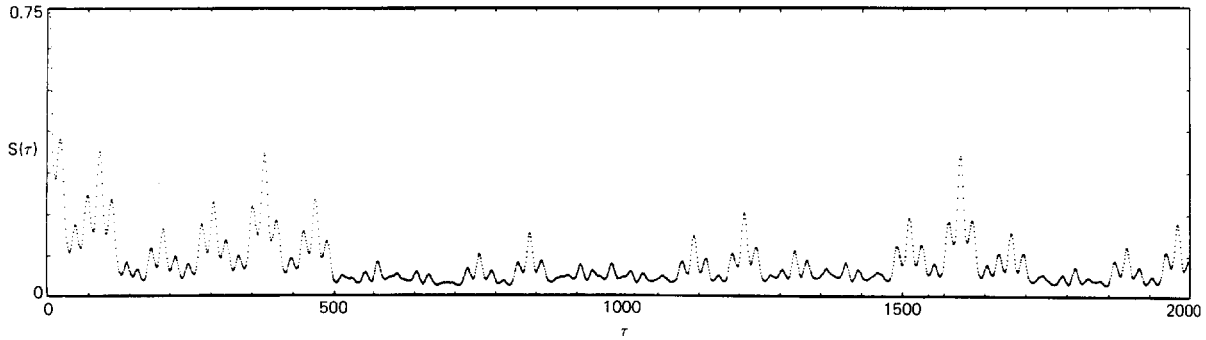

Fig. 5. The function $S(\tau)$ obtained from $|A_D(\tau)|$ by binomial smoothing. There is self-similar structure manifested by $A_D((\sqrt{5}+2)\tau) = A_D(\tau)$, and by $A_D(\alpha_n + \tau) = \frac{1}{2}A_D(\tau)$ for $\tau \ll a_n$ where $a_n = (\frac{1}{2} + 3/2\sqrt{5})\ (\sqrt{5}+2)^n$.

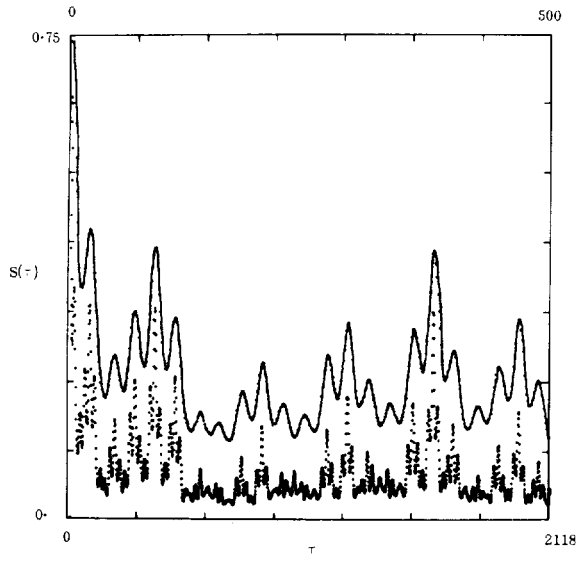

Fig. 6. Demonstration of the self-similarity $A_D((\sqrt{5}+2)\tau) = A_D(\tau)$. The smoothed data, $S(0$ to $500)$, has been displaced upward by 0.11 to separate from $S(0$ to $2118)$. The latter is compressed by $(\sqrt{5}+2)$. Note the alignment and heights of peaks in the two sets of data.

find the same phenomena at scales 1 and 5 as well as at 21, 89, etc.

The ratio of these scales is approximately $\sqrt{5}+2$ (an asymptotic result, see section 6). To dramatize the self-similarity, fig. 6 shows the result of superimposing the first 500 data points of fig. 5 with the first 2118 points of the same figure but with the abscissa reduced by the scale factor $\sqrt{5}+2$. The self-similarity is remarkably good even at these small time values!

The problem is to explain the structure we have found and be able to predict the corresponding structure for other values of the velocity ratio. It will turn out that the explanation rests on our understanding the behavior of the system for rational values of $|v_x/v_y|$. It may amuse the reader that the significance of the numbers 1, 5, 21, 89, 377, 1597, ... is not that they are every third member of the Fibonacci sequence, but rather that they are the average of twice each of the two preceeding Fibonacci numbers!

5. Rational $|v_x/v_y|$

Let us consider initial conditions such that

$$|v_x/v_y| = p/q, \tag{15}$$

where p and q are relatively prime. If the motion were restricted to a single square, the trajectory would be periodic after p bounces off the left and right walls and q bounces off the top and bottom. In terms of the time unit defined in section 3, the orbit would have period p. For motion within the 3-square system there is more than one possibility: After a time p the trajectory can return to its starting position, or it can reach one of the two equivalent positions in the other two squares (equivalent under

reflection through the square boundaries). If we call the three equivalent positions a, b, and c, there are three possible groups of mappings after the time p:

$$\begin{aligned} &G_1 \quad a \to b \to c \to a, \\ &G_2 \quad a \to b \to a;\ c \to c, \\ &G_3 \quad a \to a;\ b \to b;\ c \to c. \end{aligned} \tag{16}$$

The parity of p and q determines which of these groups is realized by the motion. It can be shown, [7], that if both p and q are odd integers, case G_1 applies; if either p or q is even, case G_2 applies; case G_3 never occurs. The cases G_1 and G_2 are illustrated in fig. 7 for the vleocity ratios $|v_x/v_y| = \frac{3}{1}$ and $\frac{2}{1}$, respectively.

In case G_1 (p and q both odd) the trajectory (and autocorrelation function) is periodic with period $3p$. The sequence $\ldots d_{j-2p}, d_{j-p}, d_j, d_{j+p}, d_{j+2p}, \ldots$ has the pattern $\ldots -1, -1, 2, -1, -1, 2, \ldots$ so that the discrete autocorrelation function at $\tau = 0, p, 2p, \ldots$ is $2, -1, -1, 2, -1$, etc.

In case G_2 (p or q is even) the period of the trajectory can be p or $2p$. If initial conditions are chosen at three equivalent points (such as a, b, c in fig. 7), two lie on the same trajectory with period $2p$ while the third lies on a trajectory with period p. We define a parameter ϵ by

$$N_1 = p\left(\frac{1}{3} - \epsilon\right), \quad N_2 = p\left(\frac{2}{3} + \epsilon\right), \tag{17}$$

where N_1 and N_2 are the number of times that the trajectory with period p, $2p$, respectively, hits the upper right wall. This parameter measures the deviation from expected linear dependence of the number of hits with the length of trajectory. It has the same value for all trajectories with the same value of $|v_x/v_y|$. Using eq. (17), the values of the discrete autocorrelation function for time differences that are integer multiples of p can easily be evaluated. The results are shown in table I. We also show in this table the weighted average of the autocorrelation function, where the weights are the trajectory lengths (i.e., $\frac{2}{3}$ for the period $2p$ trajectory and $\frac{1}{3}$ for the period p trajectory). This weighted average has applications to the irrational orbit case.

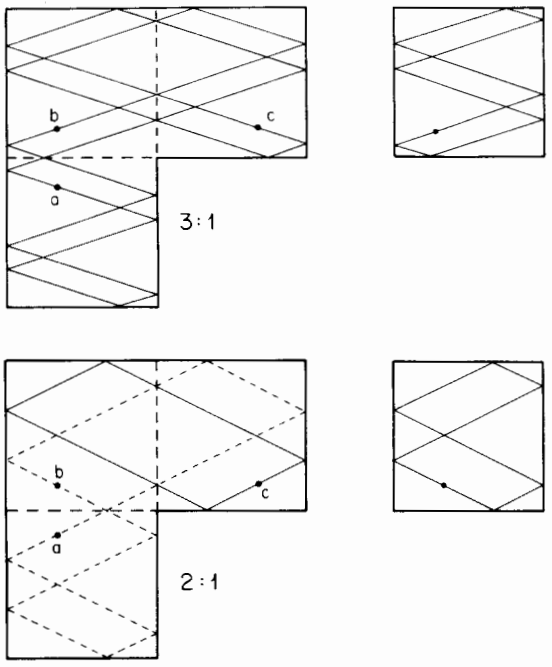

Fig. 7. The two types of periodic trajectories depending on the parities of p and q, where $|v_x/v_y| = p/q$. Trajectories in the 3-squares and in a single square are shown. Three equivalent points (a, b, c) under the mapping to the single square are shown. In the $p/q = 3/1$ = odd/odd case, a single trajectory passes through all three equivalent points. In the $p/q = 2/1$ = even/odd case, there is a trajectory (dashed) which passes through two equivalent points and another (solid) which passes through the remaining point.

TABLE I

The discrete autocorrelation function $A_D(\tau)$ for periodic orbits, $|v_x/v_y| = p/q$. For p, q = odd, even or even, odd, the average weighted by the length of the trajectory is also given. The period p trajectory hits the right side of the upper right square $(\frac{1}{3} - \epsilon)p$ times in a period

p, q		$A_D(p)$	$A_D(2p)$	$A_D(3p)$
Odd, odd		-1.00	-1.00	2.00
Odd, even / Even, odd	period p	$2.0 - 3\epsilon$	$2.0 - 3\epsilon$	$2.0 - 3\epsilon$
	period $2p$	$-1.0 - 3\epsilon$	$2.0 + \frac{3}{2}\epsilon$	$-1.0 - 3\epsilon$
	average, $\bar{A}_D$	-3ϵ	2.0	-3ϵ

6. Numerical experiments for irrational $|v_x/v_y|$

For the case that the velocity ratio is irrational, we have made a number of computer calculations of the autocorrelation function. Certain patterns can be seen in the results which can be understood on the basis of two principles:

P1) If $|v_x/v_y|$ is sufficiently close to some rational number, the autocorrelation function closely resembles that for the rational case when the time difference is not too large.

P2) A correlation that exists for time differences τ_1, τ_2, say, will cause an induced correlation at $\tau = \tau_1 \pm \tau_2$.

Part of the content of the second principle can be expressed in terms of a bound:

$$A_D(\tau_1 \pm \tau_2) \geq A_D(\tau_1) + A_D(\tau_2) - A_D(0), \tag{18}$$

where $A_D(0) = 2$. This bound is not true of autocorrelation functions in general, but it is proved for the 3-square system in the appendix. A special case of the bound when iterated is

$$A_D(n\tau) \geq 2 - n(2 - A_D(\tau)). \tag{19}$$

The rational approximations sufficiently good for the first principle to apply occur among the regular continued fraction approximations of the velocity ratio. Following the description in [8], the regular continued fraction expansion of the velocity ratio $|v_x/v_y| \equiv R$ is obtained by iteration of the relations

$$R = b_0 + \frac{1}{R_1}, \quad b_0 = \mathrm{INT}(R);$$

$$R_n = b_n + \frac{1}{R_{n+1}}, \quad b_n = \mathrm{INT}(R_n), \; n = 1, 2, 3, \ldots . \tag{20}$$

After m iterations the result is the mth convergent

$$R \approx b_0 + \cfrac{1}{b_1 + \cfrac{1}{b_2 + \cdots + \cfrac{1}{b_m}}}, \tag{21}$$

which we will denote as

$$R \approx b_0 + \left[\frac{1}{b_n}\right]_{n=1}^{m} = \frac{p_m}{q_m}. \tag{22}$$

The fractions p_m/q_m are called principal convergents, and these give the best approximations to R. The first principle works best for the principal convergents. The fractions

$$\frac{p_m^{(k)}}{q_m^{(k)}} = \frac{p_{m-2} + kp_{m-1}}{q_{m-2} + kq_{m-1}}, \quad k = 1, 2, \ldots, b_m - 1 \tag{23}$$

are called intermediate convergents. Their numerators are precisely the time differences, τ, for which the second principle applies.

To relate the behavior of the autocorrelation function for irrational velocity ratios, we define an integer ν_m to have the value $\nu_m = 2$ if either p_m or q_m is even, and $\nu_m = 3$ if they are both odd. Hence $A_D(\nu_m p_m)$ would equal 2 if $|v_x/v_y|$ were exactly equal to p_m/q_m. An analytic estimate of the "decorrelation," $2 - A_D(\tau)$, is possible. This is obtained as the product of factors which estimate the probability that the irrational trajectory passes the singular point on the opposite side to the rational trajectory. The product is

$$2 - A_D \approx \left(\frac{2}{3}\right)(\nu_m p_m)\left||v_y| - \frac{q_m}{p_m}|v_x|\right|\left(\frac{\nu_m p_m}{|v_x|}\right). \tag{24}$$

The first factor contains the decorrelation caused by passing on the wrong side of the singular point. The second factor is the number of times the trajectory passes $x = 0$. The third and fourth factors are proportional to the vertical distance, δy, that the irrational trajectory drifts from the rational trajectory: The third factor is the velocity mismatch, and the fourth factor is proportional to time (the proportionality factor has been included in the constant). This expression is written more compactly as

$$A_D \approx 2 - \frac{2}{3}(\nu_m p_m)^2\left|\left|\frac{v_y}{v_x}\right| - \frac{q_m}{p_m}\right|. \tag{25}$$

TABLE II

Each p_m/q_m is a continued fraction approximation to $|v_x/v_y|$. $\nu_m = 3$ if both p_m and q_m are odd, and $\nu_m = 2$ otherwise. The agreement between $A_D(\tau_m) \approx 2 - (2/3)\tau_m^2$ $||v_y/v_x| - q_m/p_m|$ and the numerical trajectory value is shown. The values include all the largest $A_D(\tau)$ (except $A_D(0) = 2$) for $\tau < 3000$

$\lvert v_x/v_y\rvert$	p_m	q_m	ν_m	$\nu_m p_m$	Predicted $A_D(\tau = \nu_m p_m)$	Actual $A_D(\tau)$
π	—	—	—	2	—	1.04
	3	1	3	9	1.19	1.19
	22	7	2	44	1.83	1.81
	333	106	2	666	−0.49	−0.81
	355	113	3	1,065	1.98	2.00
$1+\left[\frac{1}{n+1}\right]_{n=1}^{\infty}$	—	—	—	2	—	−0.09
	1	1	3	3	0.19	0.18
	3	2	2	6	1.25	1.16
	10	7	2	20	1.41	1.33
	43	30	2	86	1.51	1.45
	225	157	3	675	1.05	1.12
	1,393	972	2	2,786	1.63	1.42
$\frac{(\sqrt{5}+1)}{2}$	—	—	—	2	—	0.14
	1	1	3	3	−0.29	−0.29
	2	1	2	4	0.74	0.58
	3	2	2	6	0.83	0.69
	5	3	3	15	−0.71	−0.50
	8	5	2	16	0.81	0.66
	13	8	2	26	0.81	0.65
	21	13	3	63	−0.68	−0.49
	34	21	2	68	0.81	0.66
	55	34	2	110	0.81	0.65
	89	55	3	267	−0.68	−0.49
	144	89	2	288	0.81	0.65
	233	144	2	466	0.81	0.68
	377	233	3	1,131	−0.68	−0.45
	610	377	2	1,220	0.81	0.60
	987	610	2	1,974	0.81	0.52
$\frac{(\sqrt{8}+2)}{2}$	—	—	—	2	—	0.78
	2	1	2	4	1.08	0.99
	5	2	2	10	1.05	0.95
	12	5	2	24	1.06	0.96
	29	12	2	58	1.06	0.95
	70	29	2	140	1.06	0.96
	169	70	2	338	1.06	0.96
	408	169	2	816	1.06	0.94
	985	408	2	1,970	1.06	0.90
$\frac{(\sqrt{13}+3)}{2}$	—	—	—	2	—	1.09
	3	1	3	9	0.35	0.34
	10	3	2	20	1.26	1.16
	33	10	2	66	1.26	1.16
	109	33	3	327	0.34	0.31
	360	109	2	720	1.26	1.18
	1,189	360	2	2,378	1.26	1.45

Table II shows a comparison of eq. (25) with various numerical results we have obtained. When the predicted A_D value is close to 2, the agreement is excellent.

Fig. 8 illustrates an application of the principles P1 and P2 to the initial condition $|v_x/v_y| = \pi$. The autocorrelation function is large at $\tau = 9$ and $\tau = 44$ since these are $\nu_m p_m$ values corresponding to the principal convergents $p_m/q_m = \frac{3}{1}$ and $p_m/q_m = \frac{22}{7}$. The first convergent has p_m, q_m = odd, odd so that (see table I) $A_D(\tau = 3)$ is large negative. Also $A_D(\tau = 1) = -1$ from eq. (13). Then principle P2 predicts $A_D(\tau = 2)$ is large positive because $\tau = 2$ can be made as $1 + 1$ or $3 - 1$; the large value is induced by the large negative values.

The autocorrelation function can be large negative. In fact we have found from our numerical results that it takes on its largest possible negative value, $A_D = -1$, at several τ values. According to table I, we expect $A_D \approx -1$ at p_m and $2p_m$ values when p_m, q_m is odd, odd. Our experience is that $A_D = -1$ at $\tau = p_m$ often, but rarely at $\tau = 2p_m$. Finally, $A_D(\tau)$ will be large negative when $\tau = \pm\tau_1 \pm \tau_2$ where $A_D(\tau_1)$ is large positive and $A_D(\tau_2)$ is large negative. The pattern of $A_D(\tau) = -1$ values we find is such as to maximize the number of such sum or difference

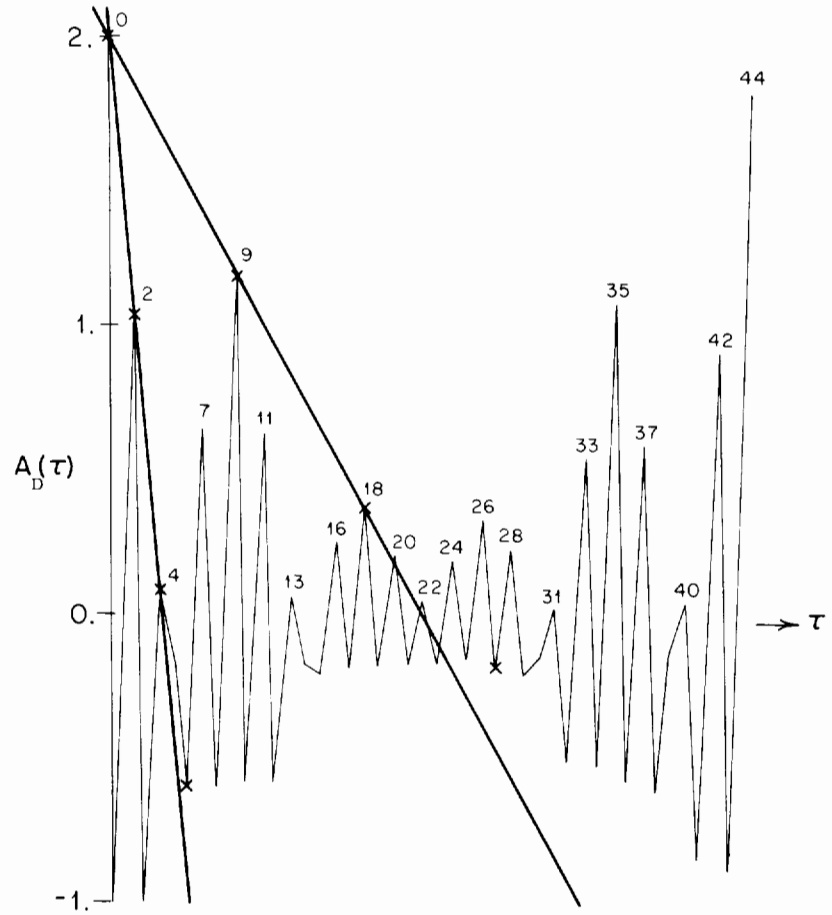

Fig. 8. $A_D(\tau)$ for $0 \leq \tau \leq 44$, shown for $|v_x/v_y| = \pi$. The heavy solid lines passing through $\tau = 0, 2, 4$ and $\tau = 0, 9, 18$ represent the lower bound, eq. (19), based on $\tau = 2$ and 9, respectively. The lines connecting successive integer values of τ do not correctly represent $A_D(\tau)$ between these points. The symmetry $A_D(44 - \tau) \approx A_D(\tau)$, following from $A_D(44) \approx A(0)$ is apparent.

combinations which can give τ; the different reasons for $A_D = -1$ mutually reinforce each other.

An application of these various rules to $|v_x/v_y| = \pi$ is shown in fig. 9. There is a strong tendency for bounds to be saturated.

The velocity ratio for which the convergents of a continued fraction expansion represent the poorest approximation is the golden mean, $|v_x/v_y| = (\sqrt{5}+1)/2$. If the considerations we have developed based on comparison with rational velocity ratios work for this value of the velocity ratio, we can be confident they will work for any other. Some of the properties of the autocorrelation function were displayed in section 4. In particular, there was seen to be a self-similar structure at scales 1, 5, 21, 89, 377, ... It turns out that these correspond to τ values where $A_D(\tau) = -1$. The continued fraction convergents for $(\sqrt{5}+1)/2$ are the ratios of adjacent Fibonacci numbers. It follows that the $\nu_m p_m$ are two or three times the Fibonacci numbers. Table II shows that the p_m, q_m = odd, odd candidates have a negative A_D value, both by the estimate and from the numerical computation of the autocorrelation function. The odd, even and even, odd candidates have a moderate positive value of A_D, but all of these are less than unity. Therefore the dominant structure in the autocorrelation function is due to the negative A_D values.

A convenient way of presenting the trends of

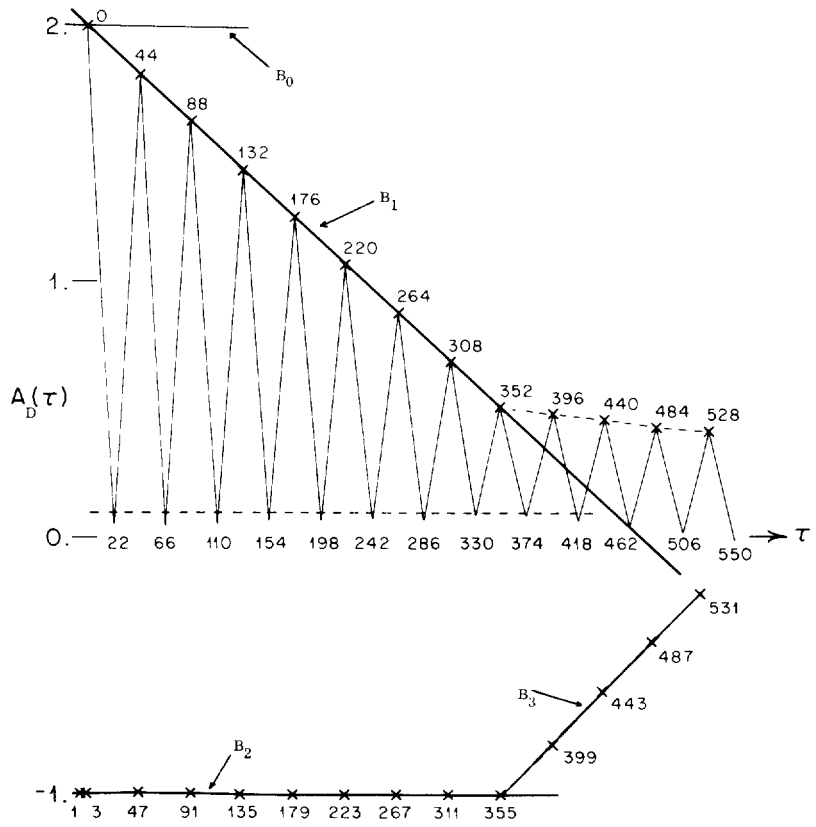

Fig. 9. $A_D(\tau)$ for $\tau = n.44$, $n.44+22$, and $n.44+3$ are shown for $|v_x/v_y| = \pi$. The solid lines are bounds: B_0, $A_D \leq 2$; B_1, $A_D(n.44) \geq n.A_D(44) - (n-1)A_D(0)$; B_2, $A_D \geq -1$; B_3, $A_D(n.44+355) \leq A_D(355) + (2 - A_D(n.44))$. The significance of the dashed line for $A_D(n.44+352)$ is simply to show that these values are colinear. The dashed line near $A_D(n.44+22)$ is the prediction $A_D \approx -3\epsilon = 0.091$, based on table I.

repeating large values of $A_D(\tau)$ is to arrange the values of τ at which the autocorrelation function is large in a "tree" diagram. On the tree "trunk" are the values $\tau = \nu_m p_m$ for which $A_D(\tau)$ is large (principle P1). Tree "branches" are made out of sums and differences of trunk values (principle P2), and "twigs" are made of sums and differences of a branch and a trunk value, etc.

For the initial condition $|v_x/v_y| = (\sqrt{5}+1)/2$, the trunk values occur at every third Fibonacci number. Since the recurrence formula for the Fibonacci number is

$$F_{m+1} = F_m + F_{m-1}, \tag{26}$$

every third such number is both a p_m value in a p_m, q_m = odd, odd pair and also the average of two adjacent $2p_m$ positive trunk values. The first explanation cannot be considered important since the corresponding $\tau = 3p_m$ value has a negative autocorrelation. The second explanation allows the reinforcement of reasons to work; for example, $89 = 68 + 21 = 110 - 21 = 377 - 288 = 466 - 377$. The tree is shown in fig. 10. The formula

$$A_D(\tau_1 \pm \tau_2) = \frac{A_D(\tau_1)A_D(\tau_2)}{A_D(0)} \tag{27}$$

works extremely well on the branches near the trunk. It continues to work well for the twigs, etc. (not shown). In fact, this golden mean velocity ratio has the remarkable property that $A_D(\tau)$ is negative for all odd values of τ and positive for all even values. The self-similar structure of figs. 4, 5, 6 and 10 is caused by the induced correlation coming from the trunk. Two adjacent Fibonacci numbers have the approximate (asymptotic) ratio $(\sqrt{5}+1)/2$. Similarly, we have $F_{m+3}/F_m \approx \sqrt{5}+2$, a result that is trivially obtained from eq. (26). It was this ratio that was used in constructing fig. 6.

The self-similar nature of the autocorrelation function is ultimately caused by the fact that the

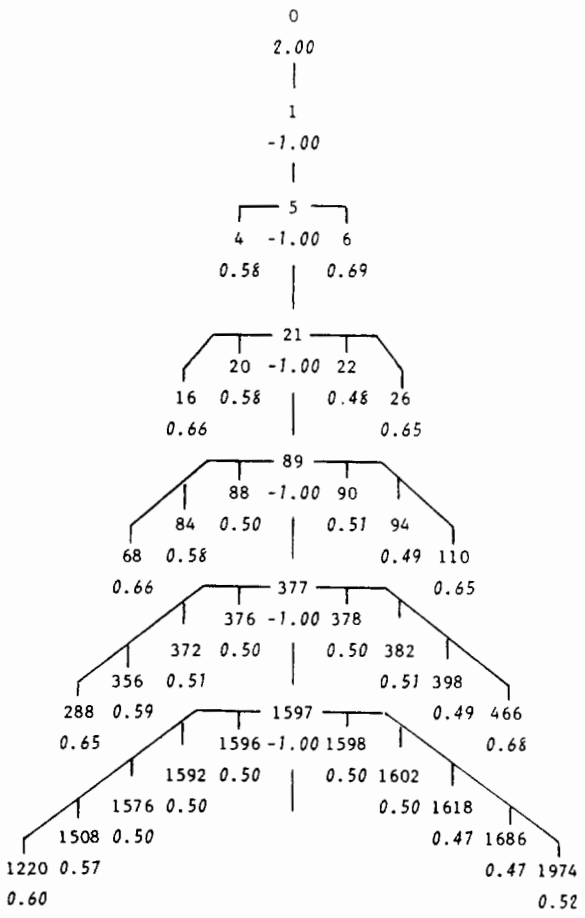

Fig. 10. The golden mean tree. Shown are both the integer τ values and the corresponding $A_D(\tau)$. The τ values on the trunk are every third Fibonacci number, and the branch tips are twice the remaining numbers.

continued fraction expansion consists of repeating denominators;

$$(\sqrt{5}+1)/2 = 1 + \left[\frac{1}{1}\right]_{n=1}^{\infty}.$$

Other velocity ratios with this property are

$$(\sqrt{8}+2)/2 = 2 + \left[\frac{1}{2}\right]_{m=1}^{\infty}$$

and

$$(\sqrt{13}+3)/2 = 3 + \left[\frac{1}{3}\right]_{m=1}^{\infty},$$

etc. both of which are considered in detail in ref. 7.

7. Summary, and Extension to Random $|v_x/v_y|$

From the examples we worked out, including those presented in section 6, we can abstract the following behavior of the discrete autocorrelation function, $A_D(\tau)$, of our pseudointegrable system:

1) If, for each principal convergent, p_m/q_m, of the continued fraction expansion of the velocity ratio $|v_x/v_y|$, we define $\nu_m = 2$ when either p_m or q_m is even, and $\nu_m = 3$ when both are odd, then the quantity

$$\tfrac{2}{3}(\nu_m p_m)^2 \left| |v_y/v_x| - q_m/p_m \right|$$

will represent a good approximation to the decorrelation, $2 - A_D(\nu_m p_m)$, if it is small. In such a case, we call $\tau = \nu_m p_m$ a positive trunk value. (Sometimes it is necessary to include $\tau = 2$ as a positive trunk value if $\tau = 3$ is a negative trunk value.) $A_D(\tau)$ takes on its largest values when τ is a positive trunk value, is somewhat smaller at branch values (defined as sums or differences of trunk values), and is smaller still at twig values (which are sums or differences of branch and trunk values). The bound, eq. (18), applies to this sequence.

2) $A_D(\tau)$ takes on its largest negative values (equal to -1) at τ values we call negative trunk values. These include $\tau = 1$; $\tau = p_m$ when p_m and q_m are both odd; and $\tau = 2p_m$ when $\tau = 3p_m$ is an extremely good positive trunk value. The remaining negative trunk values are made out of sums and differences of a negative with a positive trunk value. This usually results in negative trunk values which are half of sums or differences of adjacent negative trunk values, although other possibilities, such as the $n.44+3$ sequence for $|v_x/v_y| = \pi$, can occur.

With this understanding, and with the application of a standard result in the measure theory of continued fractions [9], it is possible to predict the nature of $A_D(\tau)$ for a randomly chosen $|v_x/v_y|$. Let us denote by r_m, the ratio of adjacent continued fraction numerators. That is,

$$r_m \equiv \frac{p_{m+1}}{p_m}. \tag{28}$$

The probability distribution of these ratios is [9],

$$P(r_m) = \frac{dr_m}{r_m(r_m+1)\ln 2}. \tag{29}$$

We wish to calculate the distribution function for ratios of positive trunk values. This requires knowledge of the distribution of ν_m values. The value of ν_m is uncorrelated with any r_n. Pairs, (ν_m, ν_{m+1}), are similarly uncorrelated with any r_n. However, sequences of more than two ν_m values are strongly correlated with r_n. For example, ν_m is completely determined once ν_{m-1}, ν_{m-2}, and the integer part of r_{m-1} are given. The probability that $\nu_m = 2$ is $\frac{2}{3}$, and the probability that $\nu_m = 3$ is $\frac{1}{3}$. Successive pairs, (ν_m, ν_{m+1}) cannot both equal 3. This information allows us to deduce the required probability distribution: Let

$$R_m \equiv \frac{\nu_{m+1} p_{m+1}}{\nu_m p_m} \tag{30}$$

denote a ratio of adjacent trunk values. Then

$$P(R_m) = \frac{dR_m}{R_m 3\ln 2}\left(\frac{1}{R_m+1} + \frac{1}{\frac{3}{2}R_m+1} + \frac{1}{\frac{2}{3}R_m+1}\right) \tag{31}$$

is the probability distribution of these ratios. Since R_m has a fixed distribution, the trunk values increase in an approximately goemetric way. In fact, for large m,

$$(\nu_m p_m)^{1/m} \approx \exp\left(\frac{\pi^2}{12\ln 2}\right) \approx 3.28, \tag{32}$$

where

$$\frac{\pi^2}{12\ln 2} = \int \ln(R_m) P(R_m) \approx 1.19. \tag{33}$$

For large τ, the number of trunk candidates with $\nu_m p_m < \tau$ is

$$N_c = \frac{1}{1.19} \ln\left(\frac{\tau}{\tau_0}\right) \tag{34}$$

where τ_0 depends on the assumed distribution of initial conditions.

A trunk candidate becomes a trunk value when its associated value of the discrete autocorrelation function is "large." The number of trunk values must depend on the definition of "large." An autocorrelation function will be called large if $A_D > 2 - a$, for some suitable a, which we assume is small. An estimate of the distribution of autocorrelation values of trunk candidates close to $A_D = 2$ can be obtained by using eq. (25), which we rewrite as (see ref. 8).

$$\begin{aligned} 2 - A_D &\approx \frac{2}{3}\nu_m^2 p_m^2 \left(\frac{1}{p_m p_{m+1}} - \frac{1}{p_{m+1} p_{m+2}} + \ldots\right) \\ &= \frac{2}{3}\nu_m^2 \frac{p_m}{p_{m+1}}\left(1 - \alpha \frac{p_m}{p_{m+1}}\right), \end{aligned} \tag{35}$$

with $0 < \alpha < 1$. If $2 - A_D$ is small, then $p_m/p_{m+1} \ll 1$; therefore

$$2 - A_D \approx \frac{2}{3}\nu_m^2 \frac{p_m}{p_{m+1}} = \frac{2\nu_m^2}{3r_m}. \tag{36}$$

Hence, the probability that $A_D > 2 - a$, given ν_m, is

$$\mathcal{P}_{a,\nu_m} = \int_{2\nu_m^2/3a}^{\infty} P(r_m)\, dr_m \approx \frac{3a}{2\nu_m^2 \ln 2}. \tag{37}$$

Averaging over $\nu_m = 2$ or 3 gives $\langle 1/\nu_m^2 \rangle = 11/54$; therefore

$$\mathcal{P}_a = \frac{11a}{36 \ln 2}. \tag{38}$$

The actual number of trunk values less than τ is therefore

$$N = N_c \mathcal{P}_a = \frac{11a}{3\pi^2} \ln\left(\frac{\tau}{\tau_0}\right). \tag{39}$$

The number of branch values less than τ for which $A_D > 2 - a$ is estimated by assuming the bound, eq. (18), is saturated. One obtains

$$2N_c^2 \int_{a_1 + a_2 \le a} d\mathcal{P}_{a_1}\, d\mathcal{P}_{a_2} = 2N_c^2 \frac{\mathcal{P}_a^2}{2} = N^2. \tag{40}$$

The number of twig values is $2N^3/3$, and in general, the number of nth generation tree values with large A_D is

$$\frac{2^{n-1}}{n!} N^n.$$

Their sum is the total number of large autocorrelation values,

$$\mathcal{N} = \tfrac{1}{2}\exp(2N) = \tfrac{1}{2}\left(\frac{\tau}{\tau_0}\right)^{22a/3\pi^2}. \tag{41}$$

Thus, the number of large autocorrelation values goes as a power of τ, where the power is proportional to the cutoff in $2 - A_D$. If we take, for example, $a = 1$, where the "small a" approximations are not very good, eq. (41) gives

$$\mathcal{N} \propto \tau^{0.7}. \tag{42}$$

We conjecture a general form for the 3-square pseudointegrable system,

$$\mathcal{N}_{\text{Pseudo}} \propto \tau^{f(a)}, \tag{43}$$

with the function $f(a)$ a monotonically rising, continuous function which satisfies $f(0) = 0$, $f'(0) = (22/3\pi^2)$, and $f(2) = 1$. This contrasts with

the behavior of integrable systems, for which the autocorrelation is an almost periodic function of τ, and

$$\mathcal{N}_{\text{Integ.}} \propto f(a)\tau. \tag{44}$$

It also contrasts with the extreme situation of a system for which the autocorrelation function decays exponentially, and

$$\mathcal{N}_{\text{Chaotic}} \propto f(a). \tag{45}$$

Acknowledgements

We would like to thank Professor Mark Kac for a helpful discussion. Financial support was provided by the La Jolla Institute and by the Department of Energy under contract No. DOE-10923.

Appendix

The bounds on $A_D(\tau)$ and $A_D(\tau_1 \pm \tau_2)$

A simple exercise in linear programming gives the desired results. Consider the function $d(t)$, eq. (4). Allowed values are $d(t) = 2$ and $d(t) = -1$. Let us denote by f_i, the fraction of d values which equal i; $f_{ij}(\tau)$ the fraction such that $d(t) = j$ and $d(t+\tau) = i$; $f_{ijk}(\tau_2, \tau_1)$ the fraction such that $d(t) = k$, $d(t+\tau_1) = j$, and $d(t+\tau_1 \pm \tau_2) = i$.

There are four fractions f_{ij} but they are constrained to satisfy

$$\left.\begin{aligned} \sum_i f_{ij}(\tau) &= f_j, \\ \sum_i f_{ij}(\tau) &= f_j, \end{aligned}\right\} \quad i, j = -1 \text{ or } 2, \tag{A.1}$$

where

$$f_2 = \tfrac{1}{3} \quad \text{and} \quad f_{-1} = \tfrac{2}{3}.$$

Three of these four constraints are independent, which means that each $f_{ij}(\tau)$, and therefore the autocorrelation function depends on a single variable, $z(\tau)$:

$$f_{22} = \frac{z}{3}, \quad f_{2-1} = f_{-12} = \frac{(1-z)}{3},$$

$$f_{-1-1} = \frac{(1+z)}{3},$$

and

$$A_D(\tau) = \sum_{ij} ij f_{ij} = 3z(\tau) - 1. \tag{A.2}$$

Each fraction is non-negative, therefore $0 \leq z \leq 1$. A_D therefore satisfies the bounds

$$-1 \leq A_D(\tau) \leq 2. \tag{A.3}$$

Similarly, there are eight fractions f_{ijk} with eight constraints:

$$\left.\begin{aligned} \sum_i f_{ijk}(\tau_2, \tau_1) &= f_{jk}(\tau_1), \\ \sum_k f_{ijk}(\tau_2, \tau_1) &= f_{ij}(\tau_2), \end{aligned}\right\} \quad i, j, k = -1 \text{ or } 2, \tag{A.4}$$

of which six are independent. Therefore, for fixed $A_D(\tau_1)$ and $A_D(\tau_2)$, f_{ijk} depends linearly on two variables. The fractions which determine the autocorrelation function of interest are

$$f_{ik}(\tau_1 \pm \tau_2) = \sum_j f_{ijk}(\tau_2, \tau_1). \tag{A.5}$$

We wish to find bounds on

$$A_D(\tau_1 \pm \tau_2) = \sum_{ik} ik f_{ik}(\tau_1 \pm \tau_2). \tag{A.6}$$

Each one of the eight f_{ijk}'s is non-negative, which restricts the allowed region of the two parameters to the interior of a polygon. Each extremum occurs at a corner of the polygon, where two of the f_{ijk}'s are zero. There are two

possibilities: The first is $A_D(\tau_1) + A_D(\tau_2) \geq 1$, for which the bound we are trying to establish is trivial since the bound $A_D(\tau_1 \pm \tau_2) \geq -1$ is at least as strong. If $A_D(\tau_1) + A_D(\tau_2) \leq 1$, the two fractions that vanish at the minimum are f_{2-12} and f_{-12-1}. This makes sense since these two fractions contribute positively to $A_D(\tau_1 \pm \tau_2)$, but negatively to both $A_D(\tau_1)$ and $A_D(\tau_2)$. Setting the two fractions equal to zero yields $A_D(\tau_1 \pm \tau_2) = A_D(\tau_1) + A_D(\tau_2) - 2$. Therefore in general, when the fractions are not necessarily zero, we have the bound

$$A_D(\tau_1 \pm \tau_2) \geq A_D(\tau_1) + A_D(\tau_2) - 2. \tag{A.7}$$

In a similar way, the upper bound is found to be

$$A_D(\tau_1 \pm \tau_2) \leq 2 - |A_D(\tau_1) - A_D(\tau_2)|. \tag{A.8}$$

The two bounds are related. For example, if $A_D(\tau_2) \leq A_D(\tau_1)$, one simply interchanges $\tau_2 \Leftrightarrow \tau_1 \pm \tau_2$.

References

[1] A.N. Zemlyakov and A.B. Katok, Mat. Zametki 18 (1975) 291 (Math. Notes 18 (1976) 760).
[2] G. Casati and J. Ford, J. Comput. Phys. 20 (1976) 97.
[3] P.J. Richens and M.V. Berry, Physica 2D (1981) 495.
[4] V.I. Arnol'd, Mathematical Methods of Classical Mechanics (Springer, New York, 1978).
[5] A. Hobson, J. Math. Phys. 16 (1975) 2210.
[6] G. Casati, F. Valz-Gris and I. Guarneri, Physica 3D (1981) 644.
[7] F.S. Henyey and N. Pomphrey, avialable as unpublished report LJI-R-81-159 (an expanded version of this paper).
[8] Encyclopedic Dictionary of Mathematics, vol. 1, S. Iyanaga and Y. Kawada eds. (MIT Press, 1977).
[9] A. Ya Khinchin, Continued Fractions (Univ. of Chicago, Chicago, 1964).